Electronic Supplementary Information

Fe_3O_4-AuNPs Anchored 2D Metal-Organic Framework Nanosheets with DNA Regulated Switchable Peroxidase-Like Activity

Bing Tan,[a] Huimin Zhao,*[a] Weihao Wu,[a] Xuan Liu,[a] Yaobin Zhang[a] and Xie Quan[a]

Key Laboratory of Industrial Ecology and Environmental Engineering (Ministry of Education, China), School of Environmental Science and Technology, Dalian University of Technology, Linggong Road 2, Dalian 116024, P. R. China

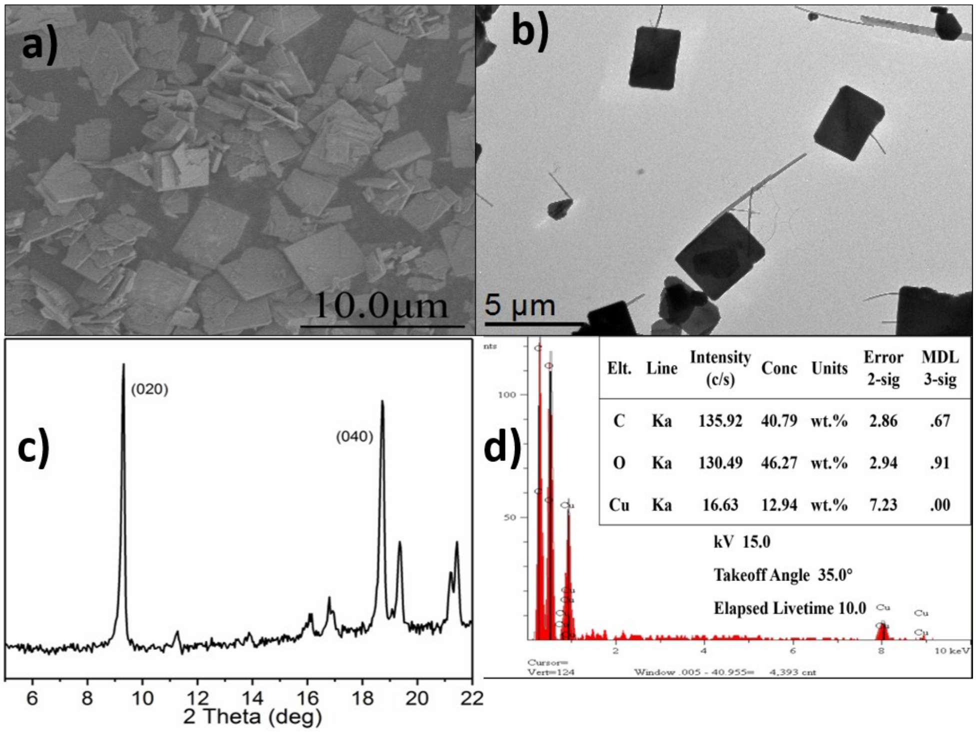

Fig. S1 a) FESEM image, b) TEM image, c) XRD pattern and d) EDS pattern of the as-synthesized Cu(HBTC)-1 nanosheets.

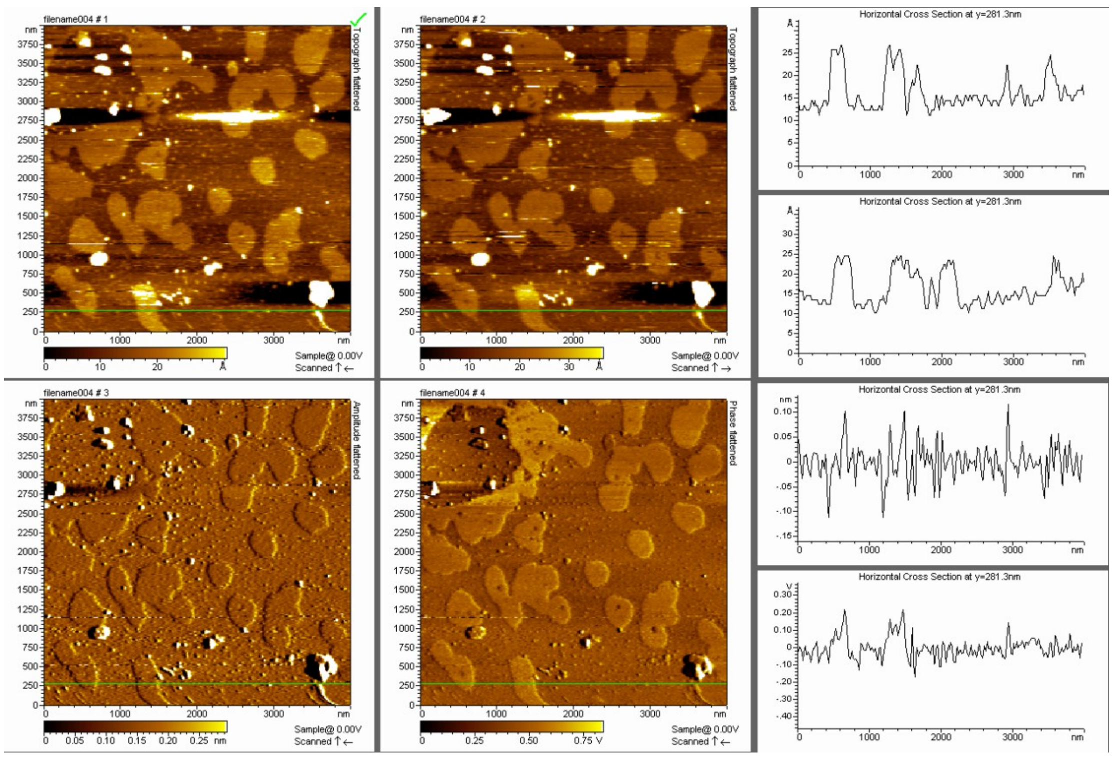

Fig. S2 AFM images and their height mode profiles of monolayer Cu(HBTC)-1/Fe_3O_4-AuNPs nanosheets on a mica plate.

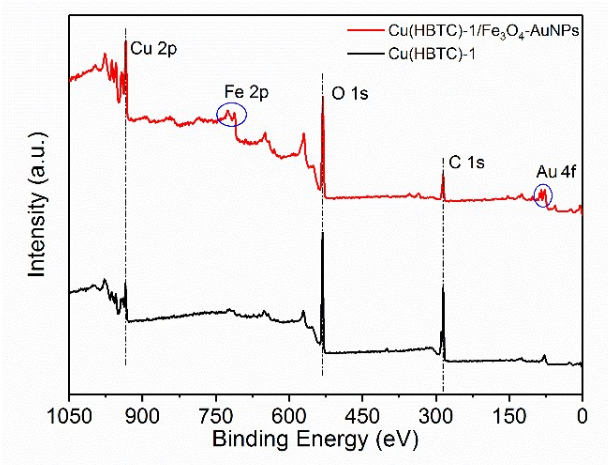

Fig. S3 XPS spectra of Cu(HBTC)-1 and Cu(HBTC)-1/Fe_3O_4-AuNPs nanosheets.

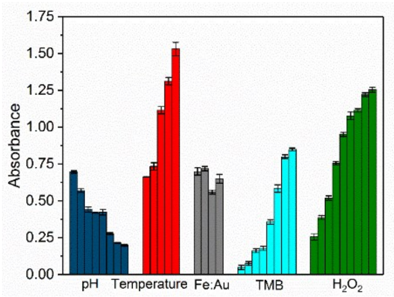

Fig. S4 Optimization of peroxidase-like catalytic conditions of Cu(HBTC)-1/Fe_3O_4-AuNPs nanosheets. Conditions (from left to right): pH = 3.6, 4.0, 4.4, 4.8, 5.2 (acetate buffer), 6.0, 7.0, 7.8 (PB buffer); reaction temperature = 25, 35, 45, 55, 65 °C; molar ratio of Fe to Au = 2.5:1, 3:1, 1:1, 1:2.5; TMB concentration = 0, 0.01, 0.03, 0.05, 0.08, 0.15, 0.50, 0.75 mM; H_2O_2 concentration = 0, 0.01, 0.02, 0.03, 0.07, 0.14, 0.36, 0.57, 0.71, 1.43 mM.

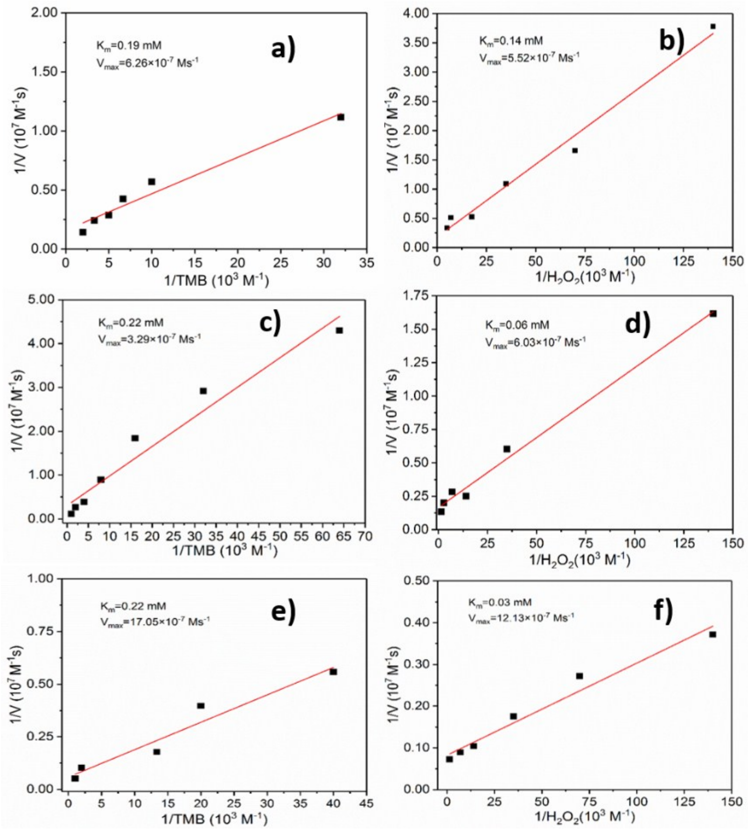

Fig. S5 The Lineweaver-Burk plots of a) and b) Cu(HBTC)-1, c) and d) Cu(HBTC)-1/AuNPs and e) and f) Cu(HBTC)-1/Fe_3O_4-AuNPs nanosheets.

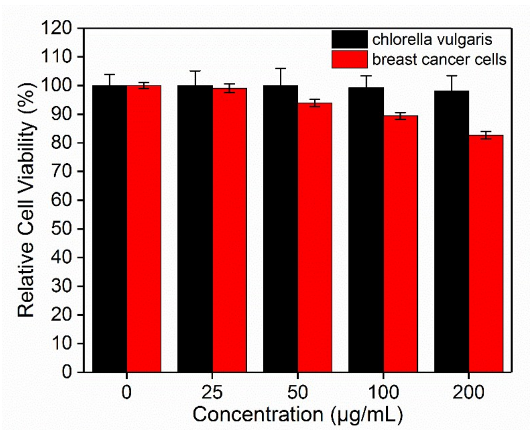

Fig. S6 In vivo toxicity of Cu(HBTC)-1/Fe_3O_4-AuNPs nanosheets. (Relative cell viability of chlorella vulgaris and breast cancer cells after incubation with different weight concentration of Cu(HBTC)-1/Fe_3O_4-AuNPs nanosheets for 24 h.)

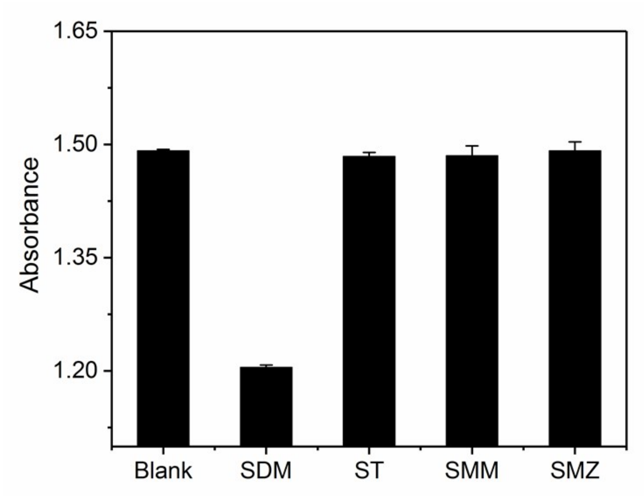

Fig. S7 Specificity study of the proposed sensor for SDM detection. The concentration of each antibiotic was 142.86 mg/mL.

Table S1 The sequences and modifications of oligonucleotides used in this work

Oligonucleotide names	Sequences (from 5' to 3') and modifications
Random 22 mer ssDNA	GAG GGC AAC GAG TGT TTA TAG A
Complementary 22 mer ssDNA	TCT ATA AAC ACT CGT TGC CCT C
FAM-22 mer ssDNA	FAM-GAG GGC AAC GAG TGT TTA TAG A
A_{22}	AAA AAA AAA AAA AAA AAA AAA A
T_{22}	TTT TTT TTT TTT TTT TTT TTT T
G_{22}	GGG GGG GGG GGG GGG GGG GGG G
C_{22}	CCC CCC CCC CCC CCC CCC CCC C
C_5	CCC CC
C_{10}	CCC CCC CCC C
C_{40}	CCC CCC CCC CCC CCC CCC CCC CCC CCC CCC CCC CCC CCC C
C_{80}	CCC CCC CCC CCC CCC CCC CCC CCC CCC CCC CCC CCC CCC CCC CCC CCC CCC CCC CCC CCC CCC CCC CCC CCC CCC CCC CC
T_5	TTT TT
T_{10}	TTT TTT TTT T
T_{40}	TTT TTT TTT TTT TTT TTT TTT TTT TTT TTT TTT TTT TTT T
T_{80}	TTT TTT TTT TTT TTT TTT TTT TTT TTT TTT TTT TTT TTT TTT TTT TTT TTT TTT TTT TTT TTT TTT TTT TTT TTT TTT TT
SDM aptamer	GAG GGC AAC GAG TGT TTA TAG A

Table S2 Comparison of kinetic parameters of previous reported peroxidase mimics.

Peroxidase mimics		substrate	K_m(mM)	V_{max}($10^{-7}Ms^{-1}$)	Reference
Cu(HBTC)-1		TMB	0.19	6.26	Present work
		H_2O_2	0.14	5.52	
Cu(HBTC)-1/-AuNPs		TMB	0.22	3.29	
		H_2O_2	0.06	6.03	
Cu(HBTC)-1/Fe_3O_4-AuNPs		TMB	0.22	15.05	
		H_2O_2	0.03	12.13	
MOFs	Hemin@MIL-101(Al)-NH_2	TMB	0.068	0.607	1
		H_2O_2	10.90	0.898	
	Fe-MIL-88NH_2	TMB	0.284	1.047	2
		H_2O_2	0.206	0.704	
	MIL-53(Fe)	TMB	1.08	0.878	3
		H_2O_2	0.04	0.186	
	Glycine-MIL-53(Fe)	TMB	0.11	0.228	4
		H_2O_2	0.10	0.225	
Transition metal dichalcogenides (TMDs) nanosheets	MoS_2 nanosheets	TMB	0.525	0.516	5
		H_2O_2	0.0116	0.429	
	MoS_2- $Pt_{74}Ag_{26}$ nanosheets	TMB	25.71	0.729	6
		H_2O_2	0.386	0.322	
	Hemin-functionalized WS_2 nanosheets	TMB	0.467	0.645	7
		H_2O_2	0.926	0.275	
	WS_2 nanosheets	TMB	1.83	0.431	8
		H_2O_2	0.24	0.452	
Graphene-based nanosheet	Carboxyl-modifie graphene oxide	TMB	0.0237	0.345	9
		H_2O_2	3.99	0.385	
	Graphene oxide/Fe_3O_4	TMB	0.43	1.308	10
		H_2O_2	0.71	0.531	
	Graphene/Au	TMB	0.29	0.56	11
		H_2O_2	274.22	2.56	
	Graphene/Fe_3O_4-Pd	TMB	0.34	2.00	12
		H_2O_2	0.02	0.558	
	3D graphene/Fe_3O_4-AuNP	TMB	0.20	4.60	13
		H_2O_2	0.20	1.50	

Table S3 Zeta potentials of Cu(HBTC)-1/Fe_3O_4-AuNPs nanosheets after incubating with different concentrations of a random 22 mer ssDNA.

ssDNA concentration (μM)	Zeta potential (mV)
No DNA	-7.16 ± 7.31
0.47	-15.1 ± 4.84
0.67	-16.4 ± 4.89
1.33	-19.8 ± 4.43

Table S4 Comparison of available methods for H_2O_2 and glucose detection based on various inorganic enzyme mimic.

Enzyme mimic	Chromogenic substrate	H_2O_2 (nM)		Glucose (μM)		Reference
		Ranges	LOD	Ranges	LOD	
Carbon dots	TMB	1000-100000	200	1-500	0.40	14
Graphene oxide	TMB	50-1000	50	1-20	1.00	9
Graphene oxide/Fe_3O_4	TMB	1000-50000	320	2-200	0.74	10
Graphene/Fe_3O_4-Pd	TMB	500-30000	86	0.50-60	0.13	12
3D graphene/Fe_3O_4-AuNP	TMB	20-190	12	0.015-0.50	0.012	13
MoS_2 nanosheets	TMB	5000-100000	1500	5-150	1.20	5
MoS_2- $Pt_{74}Ag_{26}$ nanosheets	TMB	1000-50000	400	1-10	0.80	6
Hemin-functionalized WS_2 nanosheets	TMB	5000-140000	1000	5-200	1.50	7
WS_2 nanosheets	TMB	10000-100000	1200	5-300	2.90	8
Hemin@metal-organic framework	TMB	5000-200000	2000	10-300	--	1
Cu(HBTC)-1/Fe_3O_4-AuNPs	TMB	2.86-71.43	1.10	12.86-257.14	12.20	Present work

Table S5 Comparison of available optical aptasensors for SDM detection.

Signal type	Nanomaterials	Linear range (μg/L)	LOD (μg/L)	References
Colorimetric	AuNPs	50-100	50	15
	AuNPs	--	500	16
	AuNPs	10-1000,000	10	17
	graphene/nickel@palladium hybrids	1-500	0.7	18
	Cu(HBTC)-1/Fe_3O_4-AuNPs nanosheets	3.57-357.14	1.7	Present study
Fluorescent	coordination polymer nanobelt	10-500	10	19
	graphene oxide hydrogel	25-1000	25	20

Table S6 SDM detection in natural samples and spiked recoveries.

Sample	Added (μg/L)	Detected (μg/L)	Recovery (%)	RSD (n=3)
Tap Water	75	82	113%	2.75%
	125	118	96%	1.59%
Xishan Reservoir	75	71	95%	1.06%
	125	145	116%	2.15%

References

1. F. X. Qin, S. Y. Jia, F. F. Wang, S.-H. Wu, J. Song and Y. Liu, *Catal. Sci. Technol.*, 2013, **3**, 2761-2768.
2. Y. L. Liu, X. J. Zhao, X. X. Yang and Y. F. Li, *Analyst*, 2013, **138**, 4526-4531.
3. L. Ai, L. Li, C. Zhang, J. Fu and J. Jiang, *Chem. Eur. J.*, 2013, **19**, 15105-15108.
4. W. Dong, L. Yang and Y. Huang, *Talanta*, 2017, **167**, 359-366.
5. T. Lin, L. Zhong, L. Guo, F. Fu and G. Chen, *Nanoscale*, 2014, **6**, 11856-11862.

6. S. Cai, Q. Han, C. Qi, Z. Lian, X. Jia, R. Yang and C. Wang, *Nanoscale*, 2016, **8**, 3685-3693.

7. Q. Chen, J. Chen, C. Gao, M. Zhang, J. Chen and H. Qiu, *Analyst*, 2015, **140**, 2857-2863.

8. T. Lin, L. Zhong, Z. Song, L. Guo, H. Wu, Q. Guo, Y. Chen, F. Fu and G. Chen, *Biosens. Bioelectron.*, 2014, **62**, 302-307.

9. Y. J. Song, K. G. Qu, C. Zhao, J. S. Ren and X. G. Qu, *Adv. Mater.*, 2010, **22**, 2206-2210.

10. Y. L. Dong, H. G. Zhang, Z. U. Rahman, L. Su, X. J. Chen, J. Hu and X. G. Chen, *Nanoscale*, 2012, **4**, 3969-3976.

11. M. Liu, H. Zhao, S. Chen, H. Yu and X. Quan, *ACS Nano*, 2012, **6**, 3142-3151.

12. X. J. Zheng, Q. Zhu, H. Q. Song, X. R. Zhao, T. Yi, H. L. Chen and X. G. Chen, *ACS Appl. Mater. Interfaces*, 2015, **7**, 3480-3491.

13. F. Yuan, H. Zhao, H. Zang, F. Ye and X. Quan, *ACS Appl. Mater. Interfaces*, 2016, **8**, 9855-9864.

14. W. B. Shi, Q. L. Wang, Y. J. Long, Z. L. Cheng, S. H. Chen, H. Z. Zheng and Y. M. Huang, *Chem. Commun.*, 2011, **47**, 6695-6697.

15. A. Chen, X. Jiang, W. Zhang, G. Chen, Y. Zhao, T. M. Tunio, J. Liu, Z. Lv, C. Li and S. Yang, *Biosens. Bioelectron.*, 2013, **42**, 419-425.

16. S. Niu, Z. Lv, J. Liu, W. Bai, S. Yang and A. Chen, *PLoS One*, 2014, **9**, e109263.

17. J. Yan, Y. Huang, C. Zhang, Z. Fang, W. Bai, M. Yan, C. Zhu and A. Chen,

Microchim. Acta, 2017, **184**, 59-63.

18. A. Wang, H. Zhao, X. Chen, B. Tan, Y. Zhang and X. Quan, *Anal. Biochem.*, 2017, **525**, 92-99.

19. K. M. Song, E. Jeong, W. Jeon, H. Jo and C. Ban, *Biosens. Bioelectron.*, 2012, **33**, 113-119.

20. B. Tan, H. M. Zhao, L. Du, X. R. Gan and X. Quan, *Biosens. Bioelectron.*, 2016, **83**, 267-273.